HHS Public Access

Author manuscript

Curr Genet. Author manuscript; available in PMC 2022 April 01.

Published in final edited form as:

Curr Genet. 2021 April ; 67(2): 267–281. doi:10.1007/s00294-020-01124-5.

Chromatin regulatory genes differentially interact in networks to facilitate distinct *GAL1* activity and noise profiles

David F. Moreno[1,2], **Murat Acar**[1,2,3,*]

[1]Department of Molecular Cellular and Developmental Biology, Yale University, 219 Prospect Street, New Haven, CT 06511

[2]Systems Biology Institute, Yale University, 850 West Campus Drive, West Haven, CT 06516

[3]Department of Physics, Yale University, 217 Prospect Street, New Haven, CT 06511

Abstract

Controlling chromatin state constitutes a major regulatory step in gene expression regulation across eukaryotes. While global cellular features or processes are naturally impacted by chromatin state alterations, little is known about how chromatin regulatory genes interact in networks to dictate downstream phenotypes. Using the activity of the canonical galactose network in yeast as a model, here, we measured the impact of the disruption of key chromatin regulatory genes on downstream gene expression, genetic noise and fitness. Using Trichostatin A and Nicotinamide, we characterized how drug-based modulation of global histone deacetylase activity affected these phenotypes. Performing epistasis analysis, we discovered phenotype-specific genetic interaction networks of chromatin regulators. Our work provides comprehensive insights into how the galactose network activity is affected by protein interaction networks formed by chromatin regulators.

Keywords

GAL network; GAL1; Chromatin state; Chromatin regulation; Gene expression; Noise; Yeast; TSA; Nicotinamide

Introduction

Regulation of chromatin state for initiation and progression of gene expression is a major mechanism for eukaryotic transcriptional control (Wu 1997; Luo and Dean 1999; Li et al.

*To whom correspondence should be addressed: murat.acar@yale.edu.

Author contributions

DFM and MA designed the experiments and analyses, interpreted the data and results and designed and prepared the manuscript. DFM constructed the strains, performed the experiments and collected the data. MA conceived and supervised the project.

Conflict of interests: The authors declare no competing interests.

2007). The nucleosome, composed by a histone octamer and 147bp of DNA wrapped around them, forms the basic units of the chromatin (Richmond and Davey 2003). Special protein complexes, known as chromatin regulators, can alter chromatin state by chemically modifying histone tails, relocating nucleosomes along the DNA and tuning the histone turnover (Rando and Winston 2012). These actions can be exerted locally or globally; for example, a high level of chromatin condensation is achieved during mitosis (Vas et al. 2007), while only certain gene clusters' expression are regulated by the state of their chromatin in response to external stress (Shivaswamy and Iyer 2008).

The most common chemical modifications to alter chromatin state are acetylation and methylation of the histone tails (Millar and Grunstein 2006; Bannister and Kouzarides 2011). Acetylation keeps the chromatin in a more open state, as it neutralizes the positive charges of the lysine residues and disrupts the electrostatic interactions of the histones with the DNA and usually facilitates gene expression (Bannister and Kouzarides 2011). These modifications are exerted by Histone Acetyl Transferase (HAT) and Histone DeACetylase (HDAC) enzymes, that have certain specificities for the residues they act on (Kurdistani and Grunstein 2003). The methylation reactions are relatively more complex as the modifications may occur on lysine or arginine residues, and they do not neutralize the residue's charge (Bannister and Kouzarides 2011). Arginine residues can be mono- or di-methylated, while lysine residues can be mono-, bi- or tri-methylated, producing different expression outcomes depending on the residue and its methylation load (Zhang 2001; Bannister et al. 2002); it has been shown that methylation outcomes can change during ageing (Cruz et al. 2018). Histone methylation loads are regulated by Histone Methyl Transferase (HMT) and Histone DeMethylase (HDM) enzymes (Zhang 2001; Bannister et al. 2002).

Recruitment of chromatin remodelers or transcription factors to histone modification sites leads to protein interaction hubs (Bannister and Kouzarides 2011), which can effectively be considered as intricate protein interaction networks (Lenstra et al. 2011). Nucleosome removal or relocation is performed by specific chromatin remodeling complexes upon their binding to certain histone modification marks. For example, the SWI/SNF complex displaces SAGA-acetylated histones (Chandy et al. 2006), while the INO80 complex binds DNA in the nucleosome-free regions of the transcription start sites (Yen et al. 2013).

Due to the complexity of interactions between chromatin regulators, limited information exists about how local and global phenotypes are affected by protein interaction networks formed by chromatin regulators. We have selected protein subunits belonging to key chromatin regulatory complexes and systematically studied the phenotypic consequences of their removal from the cell. As the quantitative phenotypes, we used activity and noise (as a measure of the variability in gene expression levels among isogenic cells) of the canonical *GAL1* promoter as well as vegetative growth. Despite the well-characterized nature of the *GAL1* promoter, a comprehensive characterization of its activity across different chromatin-regulatory genetic backgrounds have been missing; our work aims to address this need. We also used HDAC-inhibiting drugs to understand how these phenotypes are altered at the single-cell level. Finally, we unraveled novel genetic interactions between the regulatory components by performing epistasis analysis on data obtained from strains systematically deleted in two genes coding for the selected regulatory components.

Results

Design and construction of a single-cell level reporter system to measure gene expression and noise in selected chromatin-regulatory backgrounds

We selected six genes representing key chromatin regulators and constructed six strains by deleting these genes one at a time. The selected genes included two HMTs (SET1 (Krogan et al. 2002), SET2 (Strahl et al. 2002)) and one HDM (JHD2 (Liang et al. 2007)) acting on H3K4 (SET1, JHD2) or H3K36 (SET2), a structural component of the SWI/SNF complex (SNF6 (Cairns et al. 1994; Yoon et al. 2003)), a DNA sensor of the INO80 complex (ARP8 (Brahma et al. 2018)) and the HAT of the SAGA complex (GCN5) which acts on several lysine residues in H2B and H3 tails (Suka et al. 2001; Cieniewicz et al. 2014). The selection criteria for these genes was their being non-essential and involved in GAL network regulation (Murray et al. 2015; Lenstra et al. 2015), or their being part of major chromatin modification complexes. The base strain on which these deletions were made carried one copy of the P_{GAL1}-YFP construct integrated in the yeast genome (Acar et al. 2005, 2010; Peng et al. 2015, 2016; Elison et al. 2018; Luo et al. 2018) so that we could measure the impact of the gene deletions on gene expression and noise; flow cytometric measurement of single-cell YFP fluorescence levels led to the quantification of P_{GAL1}-YFP levels and noise (Materials and methods). To simplify the interpretation of our results, we further deleted the *GAL80* gene so that the *GAL1* promoter was constitutively active without upstream regulation or the need for galactose (Torchia et al. 1984) (Fig 1).

After constructing the strains that are deleted in chromatin regulatory genes, we first measured their vegetative growth characteristics and confirmed that the *set1Δ, snf6Δ, gcn5Δ* and *arp8Δ* had a growth defect while the *jhd2Δ* strain grew slightly better than the wildtype (Fig 2a–b), as previously described (Nislow et al. 1997; Breslow et al. 2008; Yoshikawa et al. 2011; Qian et al. 2012). However, our experimental setup allowed sufficient growth time for all strains to reach their steady state prior to further analysis.

Next, we measured P_{GAL1}-YFP expression levels in single cells and calculated gene expression noise using coefficient of variation (CV) as the metric (Fig 2c–d). We saw that the *snf6Δ* strain exhibited a major reduction (~50%) in gene expression, while it almost doubled in expression noise. Following a similar trend in expression and noise, the *arp8Δ* and *gcn5Δ* strains also exhibited a decrease in gene expression and an increase in expression noise, but in a milder fashion. On the other hand, the *jhd2Δ* strain showed a small but significant increase in gene expression with no change in noise. Finally, the *set1Δ* strain displayed a small increase in noise with no significant change in P_{GAL1}-YFP expression, while the *set2Δ* strain did not display differential phenotype compared to the wild-type.

Combining the functional roles of these chromatin regulators with the gene expression changes exerted by their absence (Fig. 2c, 2e), we propose the following model summarizing the action of these regulators on *GAL1* promoter activity. Our gene expression data support a chromatin-silencing role for Jhd2, agreeing with the previous literature (Ingvarsdottir et al. 2007). On the other hand, our data indicate that Gcn5, Snf6 and Arp8 regulators enhance P_{GAL1}-YFP expression due to a more active local chromatin state by acetylation and nucleosome displacement, as the absence of these regulators led to a decrease in reporter

expression (Fig 2e). The need for acetylation before SWI/SNF nucleosome-remodeling has been extensively studied before (Chandy et al. 2006; Chatterjee et al. 2011). SWI/SNF and INO80 (as well as RSC) share the Taf14 subunit which has high affinity to acetylated H3 and H4 nucleosomes (Shanle et al. 2015). Previous work challenged the requirement of SAGA acetylation for full GAL1 activation (Lemieux and Gaudreau 2004; Kundu et al. 2007). We note that our experimental reporter system lacks the Gal80 inhibitor; Gal80 proteins interacting with the DNA-bound Gal4 activators may have an effect on the modifications occurring on the local chromatin, potentially regulating promoter activity in the wild-type genetic background, but that is not the case in our experimental setup.

Trichostatin A decreases *GAL1* gene expression through Hos2 inhibition and improves fitness in *snf6*Δ genetic background

To obtain a deeper understanding of how chromatin regulatory proteins affect downstream gene expression and noise, we sought to quantify these phenotypes in our strains in the presence of the HDAC-inhibiting drug Trichostatin A (TSA) (Bernstein et al. 2000). To choose a sufficiently high TSA concentration not causing fitness defects due to toxicity, we measured the vegetative growth characteristics of our strains in a wide range of TSA levels. For this, we spotted serial dilutions of each strain on plates containing various TSA concentrations up to 50 μM (Fig 3a, FigS1a). We observed fitness changes for the *snf6Δ* and *set1Δ* strains, whose performance improved upon TSA treatment; for the *arp8Δ* strain, the fitness was slightly impaired by the TSA action. These phenotypes did not change much beyond the 10 μM TSA treatment (Fig 3a,3B, FigS1a). Therefore, we chose 10 μM TSA as our working concentration, which has also been the treatment concentration selected by previous studies (Bernstein et al. 2000; Wan et al. 2011).

We measured P_{GAL1}-YFP expression and noise in the wild-type and gene-deleted backgrounds after growing cells for a day in the presence of 10 μM TSA. We uniformly saw a reduction in expression, up to ~30%, in the TSA-treated strains compared to the untreated samples (Fig 3c). There was also a slight but significant increase in gene expression noise in all but the wild-type and *snf6Δ* strains; the *snf6Δ* strain likely operates in a “noise-ceiling” territory as it displayed the highest noise level across all tested strains in the absence of TSA (Fig S1b). Given the role of TSA as an HDAC inhibitor, most of the changes it elicits on cells lead to upregulated gene expression (Wan et al. 2011). Contrarily, we observed a reduction in our reporter expression, although it is known that Hos2 HDAC activity is needed for proper expression of stress-responsive and highly expressed genes such as *GAL1* (Wang et al. 2002). To rule out the possibility that the observed expression reduction upon TSA treatment was due to Hos2 activity inhibition, we deleted HOS2 and saw a reduction in P_{GAL1}-YFP expression close to the level of wild-type TSA-treated cells. However, the TSA treatment is affecting other HDAC activities beyond Hos2, as the TSA-treated *hos2Δ* exhibited further reduction in YFP expression, even though the reduction was milder compared to the one exhibited by the wild-type strain (Fig 3d). Gene expression noise on the *hos2A* strain was not altered compared to wild-type levels, either TSA-treated or not (Fig S1c).

Next, we sought to understand if the activity of the *SET2, SET1, JHD2, SNF6, ARP8, GCN5* promoters would be altered by the 10 μM TSA treatment. For this, we integrated one copy of each Promoter-YFP construct in six separate wild-type strains, with the exception of P_{JHD2}-YFP for which we integrated two copies of the construct to improve signal intensity. Measuring gene expression and noise levels after the TSA treatment, we did not observe any changes in reporter expression or noise compared to the untreated samples (Fig S3a, S3b). These results suggest that the TSA-caused changes in P_{GAL1}-YFP expression and noise in specific gene-deletion backgrounds (Fig 3c, 3d) are not mediated by changes in the expression or noise of the chromatin regulatory proteins used in our study.

To see how higher concentrations of TSA affect P_{GAL1}-YFP expression, we treated wild-type and gene-deleted strains with 25 μM and 50 μM of TSA (Fig S1d). The expression levels stabilized beyond 10 μM TSA treatment for most of the strains, except for the *arp8Δ* strain, where a dose-dependent decrease was observed. This strain has an incomplete INO80C nucleosome remodeling complex that would be expected to perform suboptimal, which may lead to a chromatin remodeling rate-limiting step in increasing TSA concentrations.

We propose the following mechanism to explain the TSA-induced gene expression reduction achieved through Hos2 inhibition (Fig 3e). While the exact mechanism causing Hos2-dependent transcriptional regulation is not known, it is known that the HDAC activity is needed for the TATA-binding protein to bind to the chromatin and also essential for RNA pol II recruitment (Sharma et al. 2007). Given the different specificities of the different HDAC enzymes, the main target sites essential to control this mechanism are the H4 tails. It is thought that Hos2 has a role in coordinating multiple rounds of transcription, which is needed for strongly inducible promoters, by resetting the chromatin acetylation balance after each passage of the RNApol II through the coding sequence (Sharma et al. 2007). Since TSA inhibits many other proteins with HDAC activities in addition to Hos2, our current work and published literature (Wang et al. 2002) indicate that Hos2 has a major role in controlling *GAL1* promoter activity.

Sirtuin inhibition by nicotinamide increases *GAL1* gene expression in an Arp8-dependent manner

Nicotinamide (NAM) acts as a potent inhibitor of the sirtuin family of NAD^+-dependent HDAC enzymes (Landry et al. 2000; Bitterman et al. 2002). To obtain further insights into how chromatin regulatory proteins affect gene expression and noise, we chose to treat wild-type and the gene-deleted strains with NAM. Using vegetative growth as a fitness indicator, we first tested the fitness of our strains in a wide range of NAM concentrations up to 50 mM (Fig 4a, Fig S2a). With the exception of the *set1Δ* mutant, we did not observe significant fitness defects as a result of the NAM treatments up to 5mM; the fitness of the *set1Δ* mutant was reduced by ~60% (Fig 4b). However, higher NAM concentrations affected the fitness of most strains (Fig 4a). We chose 5 mM NAM as our working concentration which has also been the treatment concentration selected by previous studies (Bitterman et al. 2002; Anderson et al. 2003).

We measured P_{GAL1} expression and noise in the wild-type and gene-deleted backgrounds after growing cells for a day in the presence of 5mM NAM. As expected from the role of NAM as an HDAC inhibitor, we observed a significant increase in YFP expression (despite being a small increase) in all strains except the *arp8Δ* strain (Fig. 4c). Gene expression noise stayed unchanged in all strains except in the *gcn5Δ* strain which displayed a small but significant noise reduction upon NAM treatment (Fig. 4d), which supports a model that Gcn5 proteins contribute to decreased expression heterogeneity in NAM-treated wild-type cells.

Next, we probed the activity of the *SET2, SET1, JHD2, SNF6, ARP8, GCN5* promoters under the 5mM NAM treatment to see if NAM causes any changes in promoter activity. For this characterization, we used six separate strains each carrying 1-copy integration of each Promoter-YFP cassette in the wild-type strain background; P_{JHD2}-YFP was present in two copies to increase signal intensity. We then measured gene expression and noise levels after the NAM treatment, but did not observe any changes in reporter expression or noise levels compared to the untreated samples (Fig S3a, 3b). We, therefore, propose that the NAM-caused changes in P_{GAL1}-YFP expression and noise observed in certain gene-deletion backgrounds (Fig 4c, 4d) are not mediated by changes in the expression or noise of the chromatin regulatory proteins tested.

We wanted to see how a lower NAM concentration, with less detriment on fitness especially for the *set1Δ* strain (Fig 4a), would affect P_{GAL1}-YFP expression. For this exploration, we treated wild-type and gene-deleted strains with 2mM of NAM and compared the results to the ones obtained at 5mM NAM (Fig S2b). We saw that the two NAM concentrations made similar impacts on the expression levels across the different genetic backgrounds tested.

Sirtuins are NAD^+-dependent HDAC enzymes that silence chromatin, mainly by removing acetyl groups from H3K9 and H4K16 which are hallmark facilitators of chromatin compaction (Martínez-Redondo and Vaquero 2013). Considering the inhibitory role of NAM on sirtuins, our observation of an increase in the P_{GAL1}-YFP expression after the NAM treatment (Fig 4c) fits into a straightforward mechanistic framework. Interestingly, the NAM-caused P_{GAL1}-YFP expression we measured in the *arp8Δ* background did not fit into this framework. Our results indicate a need for Arp8 as a component of the INO80 chromatin-remodeling complex to efficiently displace the acetylated nucleosomes to promote higher gene expression levels when cells are treated with NAM (Fig 4e).

Discovery of phenotype-specific genetic interaction networks of chromatin regulators

As chromatin regulator activity can be expected to require multiple enzymes or protein complexes, it is plausible to hypothesize for the presence of an interaction network among the chromatin regulators we selected. To uncover the interaction type and strength between each regulator pair, we combinatorically deleted two of five genes in the same strain, measured the resulting phenotypes of growth, expression and noise, and compared them to the phenotypic levels obtained from the strains missing only one of the two genes in a single strain. As the *set2Δ* strain did not show major phenotypic differences in comparison to the wild type in our previous characterizations (Fig. 2), *set2Δ* was not included in our network discovery efforts and a total of ten double-deletion strains were constructed out of the five

chromatin regulator genes. We measured genetic interaction type and strength by considering a product-based epistasis model as the neutral model (see Materials and Methods). Most genetic interaction screens (Boone et al. 2007; Costanzo et al. 2016; van Leeuwen et al. 2017) published previously extract interaction maps based on the use of global phenotypes such as growth or fitness; in this work, in addition to using probes such as growth, we use locus-specific gene expression and noise to dissect the local downstream impact of key chromatin regulatory proteins over the *GAL1* promoter activity.

We measured vegetative growth of our double-deletion strains using a spotting assay on solid media (Fig 5a, Fig S4b), and detected major growth defects, compared to the wild type growth, especially in the *set1Δsnf6Δ, set1Δarp8Δ, arp8Δgcn5Δ, gcn5Δset1Δ* and *gcn5Δsnf6Δ* genetic backgrounds; however, the *jhd2Δarp8Δ* strain outperformed the wild-type. A majority of the double gene-deleted strains performed significantly worse than their single gene-deleted counterpart strains, except in the *jhd2Δsnf6Δ* and *jhd2Δarp8Δ* strains where *JHD2* deletion improved the fitness of *snf6Δ* and *arp8Δ* strains (Table S2). When we performed an epitasis analysis on our results, we detected interactions, either positive or negative, between all nodes of our network, except between *SET1* & *ARP8* and *GCN5* & *SNF6* (Fig 5b, Table S5), which had not been detected in previous genome-wide screening studies (Collins et al. 2007; Costanzo et al. 2016).

Comparing P_{GAL1}-YFP expression in the five double gene-deleted strains with the one in the wild type strain, we detected a mild increase in expression in the *jhd2Δarp8Δ* strain but a massive reduction in expression in the *gcn5Δsnf6Δ* strain which was even stronger than the reductions we observed in the strain's single gene-deleted counterparts (Fig 5c, Table S3). Performing epistasis analysis, we detected significant positive and negative interactions between all genetic nodes composing the chromatin regulatory network dictating P_{GAL1}-YFP expression, including the gain of function detected when *jhd2Δ* and *arp8Δ* deletions were combined, the loss of function detected when *gcn5Δ* and *snf6Δ* deletions were combined, and the partial gain of function effect of the arp8Δ deletion over the *snf6Δ* deletion (Fig 5d, Table S5).

For noise in gene expression, compared to the wild-type, the largest synergistic increases were detected when the noisiest single gene-deleted strains *snf6Δ, arp8Δ* and *gcn5Δ* were combined in a single strain. On the other hand, deleting any of those genes in *jhd2Δ* background led to significant noise reduction compared to the strains carrying the single gene deletions with a functional *JHD2* gene (Fig 5e, Table S4). With respect to the genetic noise interactions discovered (Fig 5f, Table S5), we uncovered positive interactions between *GCN5* & *ARP8, GCN5* & *SNF6* and *SET1* & *JHD2.* On the other hand, we have found significant negative interactions between most of the other gene pairs analyzed, especially between *ARP8* and *SNF6*. There was no significant interaction between *SET1* and *GCN5.*

We were interested in identifying potential interconnections between the phenotypes we have measured. For our single- and double-mutant strain sets, we computed the deviations from the wild-type phenotypes (after normalization with respect to the wild type), and calculated the correlations between the resulting phenotypic values (Fig. 6a–c). We found significant negative correlations between reporter expression and expression noise and

between vegetative growth and expression noise (Fig. 6a, 6c). On the other hand, there was a positive correlation between vegetative growth and reporter expression (Fig. 6b). The correlations between phenotypes measured in the single gene-deleted strains were stronger than the ones measured in the double gene-deleted strains; this may be because the removal of multiple components of the network leads to a diminished control over the chromatin regulation function compared to when just one component is removed. The negative correlation between reporter expression and noise suggests that the same mechanism ensuring high *GAL1* expression also keeps the expression levels less heterogeneous. The positive correlation detected between reporter expression and vegetative growth suggest that the mutants displaying reduced reporter expression also experienced an expression reduction on genes related to the growth processes, leading to a growth defect.

Using Gene Set Enrichment Analysis (GSEA) on the expression profiles obtained from a previously published microarray transcriptome dataset comprising deletion mutants of most of the chromatin modifier genes (Lenstra et al. 2011), we found that the most upregulated gene set in the *jdh2Δ* background was the category of 'ribonucleoprotein complex biogenesis'; in our study, the *jdh2Δ* background displayed the highest reporter expression and vegetative growth. At the same time, the same gene set was identified as the most downregulated gene set in the *snf6Δ* genetic background (Fig 6d, 6e, Table S6). The *jdh2Δ* and *snf6Δ* strains constitute the extreme points of the growth vs. expression correlation. The published dataset did not include the GAL network genes and their experiments were not done in GAL network-inducing conditions; nevertheless, coupled with our data, GSEA results indicate that the GAL network and the ribosome biogenesis network are coordinately regulated.

Discussion

Overall, our results describe how the lack of key chromatin regulator agents affects galactose network activity and noise, as well as global fitness in the yeast *Saccharomyces cerevisiae.* Also, our work sheds light on the phenotypic consequences of treating yeast cells with two frequently-used HDAC inhibiting drugs, followed by mechanistic explanations of their effects. Finally, by combining gene deletions in single strains, we unravel genetic interactions between the key chromatin regulators with respect to the phenotypes assayed.

Our results highlight the importance of the chromatin regulation and histone modification in tuning the GAL network activity, even in conditions where the amount of well-positioned nucleosomes in the assayed promoter region is minimal, as it is the case on the P_{GAL1} region when the strain lacks the *GAL80* inhibitor (Bryant et al. 2008). A strong expression defect was detected when the SWI/SNF complex was disrupted, likely due to the fact that the nucleosome occupancy of the *GAL1* promoter is not fully cleared in inducing conditions (Bryant et al. 2008). This was accompanied by a major increase in cell-to-cell expression heterogeneity, as the defective SWI/SNF complex is not expected to respond as precisely and consistently as the full complex across the cell population.

The product of the enzymatic reaction catalyzed by the Gal1 galactokinase is toxic to yeast cells unless it is processed by the Gal7 and Gal10 enzymes (Mumma et al. 2008). Therefore,

there is an evolutionary pressure for establishing a regulatory mechanism facilitating similar *GAL1* and *GAL10* expression. *GAL10* gene codes for a UDP-glucose-4-epimerase. Separated by a common intergenic region, *GAL1* and *GAL10* are encoded in opposite directions and it is known that they are expressed at similar levels in the wild-type genetic background (Elison et al. 2018). The definitive answer to the question of whether or not the *GAL1-GAL10* expression balance would still hold in the *gal80Δ* background would need further experiments. Since the chromatin over the *GAL10* region is trimethylated by Set1 in GAL network-repressive conditions (Houseley et al. 2008), the use of glucose might affect the *GAL1–GAL10* expression balance in the *set1Δ* strain; however, this is not relevant to us as a way to cause imbalance between *GAL1* and *GAL10* expression because we do not use glucose in this study.

The observed TSA-induced expression downregulation we measured across all our strains is likely specific to the Hos2-activated promoters (e.g. stress-related promoters or strongly-inducible promoters such as P_{GAL1}), as the TSA treatment upregulates gene expression across the genome by inhibiting HDAC activities (Wan et al. 2011). Hos2-mediated expression activation is thought to be accomplished by deacetylation of the H4 tails, as a mechanism to recruit RNApol II to these promoters and reset the chromatin state after a RNApol II passage to enable multiple and coordinated transcription rounds (Sharma et al. 2007).

The NAM-mediated increase in gene expression due to the extra acetylation caused by the sirtuin HDAC inhibition was dependent of the INO80 complex component Arp8, suggesting that this chromatin remodeler needs the sirtuin-controlled H3K9 and H4K16 in the acetylated state to be remodeled towards promoting more efficient gene expression. Arp8 has a critical role for the initial formation of INO80-to-chromatin interactions (Zhang et al. 2019), and it has been shown by ChIP experiments that there was a significant correlation between many histone acetylation marks and Arp5 genome occupancy, with Arp5 being another INO80 component (Beckwith et al. 2018). On the other hand, the high sensitivity towards the treatment concentration, as observed in the *set1Δ* strain, may be due to a synergistic effect between the extra NAM-induced acetylation and the lack of H3K4me3-dependent activity of the Rpd3L complex, leading to a hyperacetylated state as in cells in a stationary culture (Weinert et al. 2014).

The genetic interactions we have found, except for the *SET1-JHD2* pair (Soloveychik et al. 2016), had not been previously reported, although interactions between other components of the same complexes have been known (Hassan et al. 2002; Barbaric et al. 2007; Costanzo et al. 2016). Also, rather than drawing conclusions based on global fitness changes affected by genetic perturbations, we have discovered the new interactions based on changes in local reporter expression phenotypes, which gives more direct insights into the chromatin regulator factors' effect on downstream phenotypes. Moreover, we have observed correlations among vegetative growth, reporter expression and expression noise, showing the effect of chromatin regulators on the interplay between these phenotypes.

Our previous work has shown that cells undergo a decrease in cell-intrinsic P_{GAL1} noise during aging, and the absence of the Rpd3 HDAC protein modifies this noise trend by also

increasing replicative lifespan (Liu et al. 2017). Building on the results from our previous and current work, systematically deleting from the yeast genome additional chromatin-regulatory factors and tracking their impact on gene expression, cell-intrinsic noise and replicative lifespan will provide a broader understanding on why there are cell-to-cell variations in ageing speeds and single-cell lifespans despite the isogenic nature of the starting cellular states.

Materials and methods

Construction of plasmids and yeast strains

All *S. cerevisiae* strains used in this study are Matα haploids which are related to the BY genetic background. Detailed descriptions of strain genotypes can be found in Table S1. The WP190 strain, in which the *GAL80* gene is deleted, carries a P_{GAL1}-YFP reporter integrated in the *ho* locus (Liu et al. 2017). We generated yeast strains deleted in *SET2, SET1, JHD2, SNF6, ARP8, GCN5*, or *HOS2* open reading frames (ORFs) by PCR-amplifying the ScURA3 marker from pRS306 plasmid with primers containing 60bp sequences homologous to the regions flanking the targeted ORF and transforming the PCR products into the WP190 strain; the transformed colonies were selected on SCD-Ura plates and confirmed by PCR (the *HOS2* ORF was deleted with the ScLEU2 marker, amplified from pRS305 plasmid, and colonies were selected on SCD-Leu plates). The double gene-deleted strains were constructed similarly, this time PCR-amplifying the ScLEU2 marker from pRS305 plasmid with primers containing 60bp sequences homologous to the regions flanking the targeted ORF and transforming a single gene-deleted strain with the PCR product; the transformed colonies were selected on SCD-Ura-Leu plates and confirmed by PCR.

Using as backbone a plasmid carrying a SpHis5 marker and P_{GAL1}-YFP followed by a CYC terminator (Liu et al. 2017), we cloned P_{SET2}, P_{SET1}, P_{JHD2}, P_{SNF6}, P_{ARP8} or P_{GCN5} in place of the P_{GAL1} by PCR-amplifying the whole upstream intergenic region before each corresponding gene; KpnI and BamHI sites were present on both sides of the P_{GAL1} and they were also added in the PCR primers to amplify the various promoters mentioned above. Then, we PCR-amplified the whole above-mentioned plasmid except the P_{GAL1} region, digested the PCR product with BamHI, KpnI and DpnI (to digest the template) and ligated the digested product to the BamHI-KpnI-digested promoters using the T4 DNA ligase. After the ligation, DNA was transformed into *E. coll* and the recombinant plasmids were checked by PCR and confirmed by sequencing. These new plasmids were used as template to PCR-amplify SpHis5-P_{xxx}-YFP-CYCt and integrate these products into the *ho* locus of the AL002 strain; during the PCR-amplification, we used primers containing 60bp sequences homologous to the *ho* locus. A second copy of P_{JDH2}-YFP was needed to increase the signal, so we integrated it into the *ura3* locus of the strain already bearing one copy of the P_{JHD2}-YFP reporter at the *ho* locus. For this, we substituted the SpHIS5 marker from the original plasmid with a ScURA3 marker. We amplified the whole P_{JHD2}-YFP-containing plasmid except the SpHIS5 marker (adding a HindIII site and containing a KpnI site at the other end); the ScURA3 marker was amplified from pRS306 plasmid with primers containing the same restriction sites. Both PCR products were digested with KpnI, HindIII

and Dpnl (to digest the template) and T4-ligated. Afterthe ligation, DNA was transformed into *E. coli* and the recombinant plasmids were checked by PCR and confirmed by sequencing. This plasmid was used as a template for ScURA3-P_{JHD2}-YFP-CYCt amplification and the resulting PCR product was integrated into the *ura3* locus of the strain already bearing one copy of the P_{JHD2}-YFP reporter in the *ho* locus; during the PCR-amplification, we used primers containing 60bp sequences homologous to the *ura3* locus.

Growth conditions and media

For vegetative growth measurements, cells were grown in a shaker incubator (30°C, 225rpm) in synthetic complete media with 2% glucose (SCD) until exponential phase was reached in 5ml (OD_{600}~0.2–0.3). After measuring the cell densities, all cultures were adjusted to OD_{600}=0.2 and 200μl from the cultures were transferred to a well in a 96-well plate. Serial dilutions (1:10) were made on neighboring wells of the same plate and they were spotted onto SCD agar plates with a 6×8 replica plater (Sigma). To prepare the drug-containing plates (with TSA or NAM), proper volumes from the stock solutions (for TSA at 10mM in ethanol, for NAM at 2M in H_2O) were added to the agar plate media when it cooled down to~60´C, and then it was mixed and poured. After spotting, the plates were incubated for 2 days at 30°C and photographed afterwards.

For cytometry-based measurements, by always keeping the OD_{600} below 0.2 to prevent nutrient depletion, cells were grown overnight in a shaker incubator (30°C, 225 rpm) in synthetic complete media with 0.1% mannose (SCM) in 5ml volume, then they were diluted and grown for 23 h in the same media (overnight growth phase). Then, the cells were again diluted and grown in the same media (plus drug if needed) for another 23 h (induction phase). Subsequently, cells were washed and suspended in 500 μl of PBS and kept on ice prior to measurement.

Single-colony area measurement

Single-colony areas were quantified from plate pictures using ImageJ (Wayne Rasband, NIH). First, a section of the image corresponding to a particular strain was cropped; then, it was thresholded to highlight the area containing colonies and binarized. Then, single colonies were resolved from their neighbors by a watershed algorithm, and filtered by criteria based on size and circularity. This process was semi-automated by the use of an ImageJ macro (see Supplementary Information) and refined by visual inspection. When comparing different strains grown on SCD media, we normalized all phenotypic values to the wild-type strain’s mean value for each phenotype, and then calculated the Log2 of this ratio. In the drug treatment experiments, all values were normalized to each strain’s mean colony size value measured on SCD plates not containing the drug. We combined measurements from 2 to 4 plates in order to calculate mean values for each of our independent biological replicates. 3–5 biological replicates were made, leading to the calculation of the mean of means and the SEM (for error bars). For statistical analysis, we made pairwise t test comparisons between the wild-type and the gene-deleted strains’ phenotypic values, or between conditions with and without drug treatment.

Flow cytometry

Flow cytometry measurements were performed using a FACSVerse (Beckton Dickinson). We measured 10000 events for each strain and condition (except for the *Δgcn5Δsnf6*, where 30000 events were measured). Raw data were converted to CSV files with FCSExtract 1.02 (Earl F. Glynn, Stowers Institute), and followed by custom analyses performed on spreadsheets. For YFP fluorescence measurements, a small FSC-SSC gate was consistently placed on the densest region (corresponding to ~20% of all events) to avoid cell-size-based variations. A threshold for ON state was established by choosing a YFP signal level greater than the mean+4SD of the autofluorescence measured from the control strain not carrying any reporter proteins. Using the ON-gated cells, we calculated the mean YFP expression and its noise (measured as the CV of the single-cell YFP expression levels) for each biological replicate. When comparing different strains grown in SCM media, we normalized the measured phenotypic values to the wild-type strain's mean value for each phenotype, and then calculated the Log2 of this ratio. When comparing gene expression between drug-treated conditions, we used the non-normalized values. 2–5 biological replicates were obtained, from which we calculated the mean of means and the SEM (for error bars). For statistical analysis, we made pairwise t test comparisons between the wild-type and the gene-deleted strains' phenotypic values, or between conditions with and without drug treatment.

Identification of genetic interactions

We scored a genetic interaction between a pair of genes (*x,y*) for a specific phenotype when the phenotype (W_{xy}) measured from the double gene-deleted strain diverged significantly from the product of the phenotypes ($W_x * W_y$) measured from each of the single gene-deleted strains, with the equality between (W_{xy}) and (W_{xy} indicating that the genes are not interacting based on the product-based epistasis model. Computations were performed as described previously (Onge et al. 2007). Briefly, we normalized the phenotypic values by the wild-type phenotypes, calculated the $W_x * W_y$ mean and SD approximated by the delta method, and tested for the significance of the difference between the W_{xy} and the $W_x * W_y$ using a Z test. Interactions were scored if the resulting p-value was less than 0.01. Depending on the sign of the subtraction ($W_{xy} - W_x * W_y$), we defined the interactions as positive if the subtraction was positive or negative if it was negative (Fig S4a).

Gene set enrichment analysis (GSEA) using microarray data

Gene expression ratio data (Log_2 of fold-change ratio between gene-deleted and wild-type strain) was obtained from a previously published study (www.holstegelab.nl/publications/chromatin_regulators; Lenstra et al. 2011). Data were visualized with JavaTreeView (Saldanha 2004) by following the authors' instructions, from which we extracted and exported the fold-change expression data related to our six gene-deleted strains of interest. We used the [Gene_Name – Fold Change] output list as input for performing GSEA using WebGestalt (Liao et al. 2019, www.webgestalt.org/), selected *Saccharomyces cerevisiae* as organism of interest, selected GSEA as analysis method and 'geneontology / Biological Process' as functional database, keeping the rest of the advanced parameters at their default levels (except using False Discovery Rate (FDR)<0.05 to determine the significance

threshold to select the gene sets displayed). From the [Gene_Name – Fold Change] output list, we manually deleted the row representing the deleted gene, which expectedly had the largest negative score that could affect the downstream outcome. Afterwards, similar gene sets were clustered by selecting the 'Affinity Propagation' option for the display of the final tables and bar plots.

Supplementary Material

Refer to Web version on PubMed Central for supplementary material.

Acknowledgements

We thank M. Aldea for comments on the manuscript, the Acar Lab members for helpful discussions, and K. Nelson for cytometry technical assistance. MA acknowledges funding from the National Institutes of Health (R01GM127870 and U54CA209992). The funding bodies did not play any roles in the design of the study and collection, analysis, and interpretation of data and in writing the manuscript.

REFERENCES

Acar M, Becskei A, van Oudenaarden A (2005) Enhancement of cellular memory by reducing stochastic transitions. Nature 435:228–232. 10.1038/nature03524 [PubMed: 15889097]

Acar M, Pando BF, Arnold FH, et al. (2010) A General Mechanism for Network-Dosage Compensation in Gene Circuits. Science 329:1656–1660. 10.1126/science.1190544 [PubMed: 20929850]

Anderson RM, Bitterman KJ, Wood JG, et al. (2003) Nicotinamide and PNC1 govern lifespan extension by calorie restriction in Saccharomyces cerevisiae. Nature 423:181–185. 10.1038/nature01578 [PubMed: 12736687]

Bannister AJ, Kouzarides T (2011) Regulation of chromatin by histone modifications. Cell Res 21:381–395. 10.1038/cr.2011.22 [PubMed: 21321607]

Bannister AJ, Schneider R, Kouzarides T (2002) Flistone Methylation. Cell 109:801–806. 10.1016/S0092-8674(02)00798-5 [PubMed: 12110177]

Barbaric S, Luckenbach T, Schmid A, et al. (2007) Redundancy of Chromatin Remodeling Pathways for the Induction of the Yeast PFI05 Promoter in Vivo. J Biol Chem 282:27610–27621. 10.1074/jbc.M700623200 [PubMed: 17631505]

Beckwith SL, Schwartz EK, García-Nieto PE, et al. (2018) The INO80 chromatin remodeler sustains metabolic stability by promoting TOR signaling and regulating histone acetylation. PLOS Genet 14:e1007216. 10.1371/journal.pgen.1007216 [PubMed: 29462149]

Bernstein BE, Tong JK, Schreiber SL (2000) Genomewide studies of histone deacetylase function in yeast. Proc Natl Acad Sci U S A 97:13708–13713. 10.1073/pnas.250477697 [PubMed: 11095743]

Bitterman KJ, Anderson RM, Cohen HY, et al. (2002) Inhibition of Silencing and Accelerated Aging by Nicotinamide, a Putative Negative Regulator of Yeast Sir2 and Human SIRT1. J Biol Chem 277:45099–45107. 10.1074/jbc.M205670200 [PubMed: 12297502]

Boone C, Bussey H, Andrews BJ (2007) Exploring genetic interactions and networks with yeast. Nat Rev Genet 8:437–449. 10.1038/nrg2085 [PubMed: 17510664]

Brahma S, Ngubo M, Paul S, et al. (2018) The Arp8 and Arp4 module acts as a DNA sensor controlling INO80 chromatin remodeling. Nat Commun 9:3309. 10.1038/s41467-018-05710-7 [PubMed: 30120252]

Breslow DK, Cameron DM, Collins SR, et al. (2008) A comprehensive strategy enabling high-resolution functional analysis of the yeast genome. Nat Methods, 10.1038/nmeth.1234

Bryant GO, Prabhu V, Floer M, et al. (2008) Activator Control of Nucleosome Occupancy in Activation and Repression of Transcription. PLoS Biol 6:e317. 10.1371/journal.pbio.0060317

Cairns BR, Kim YJ, Sayre MH, et al. (1994) A multisubunit complex containing the SWI1/ADR6, SWI2/SNF2, SWI3, SNF5, and SNF6 gene products isolated from yeast. Proc Natl Acad Sci U S A 91:1950–1954. 10.1073/pnas.91.5.1950 [PubMed: 8127913]

Chandy M, Gutierrez JL, Prochasson P, Workman JL (2006) SWI/SNF Displaces SAGA-Acetylated Nucleosomes. Eukaryot Cell 5:1738–1747. 10.1128/EC.00165-06 [PubMed: 17030999]

Chatterjee N, Sinha D, Lemma-Dechassa M, et al. (2011) Flistone H3 tail acetylation modulates ATP-dependent remodeling through multiple mechanisms. Nucleic Acids Res 39:8378–8391. 10.1093/nar/gkr535 [PubMed: 21749977]

Cieniewicz AM, Moreland L, Ringel AE, et al. (2014) The Bromodomain of Gcn5 Regulates Site Specificity of Lysine Acetylation on Histone H3. Mol Cell Proteomics 13:2896–2910. 10.1074/mcp.M114.038174 [PubMed: 25106422]

Collins SR, Miller KM, Maas NL, et al. (2007) Functional dissection of protein complexes involved in yeast chromosome biology using a genetic interaction map. Nature 446:806–810. 10.1038/nature05649 [PubMed: 17314980]

Costanzo M, VanderSluis B, Koch EN, et al. (2016) A global genetic interaction network maps a wiring diagram of cellular function. Science 353:aaf1420. 10.1126/science.aaf1420 [PubMed: 27708008]

Cruz C, Della Rosa M, Krueger C, et al. (2018) Tri-methylation of histone H3 lysine 4 facilitates gene expression in ageing cells. eLife 7:. 10.7554/eLife.34081

Elison GL, Xue Y, Song R, Acar M (2018) Insights into Bidirectional Gene Expression Control Using the Canonical GAL1/GAL10 Promoter. Cell Rep 25:737–748.e4. 10.1016/j.celrep.2018.09.050 [PubMed: 30332652]

Hassan AH, Prochasson P, Neely KE, et al. (2002) Function and Selectivity of Bromodomains in Anchoring Chromatin-Modifying Complexes to Promoter Nucleosomes. Cell 111:369–379. 10.1016/S0092-8674(02)01005-X [PubMed: 12419247]

Houseley J, Rubbi L, Grunstein M, et al. (2008) A ncRNA Modulates Histone Modification and mRNA Induction in the Yeast GAL Gene Cluster. Mol Cell 32:685–695. 10.1016/j.molcel.2008.09.027 [PubMed: 19061643]

Ingvarsdottir K, Edwards C, Lee MG, et al. (2007) Histone H3 K4 Demethylation during Activation and Attenuation of GAL1 Transcription in Saccharomyces cerevisiae. Mol Cell Biol 27:7856–7864. 10.1128/mcb.00801-07 [PubMed: 17875926]

Krogan NJ, Dover J, Khorrami S, et al. (2002) COMPASS, a Histone H3 (Lysine 4) Methyltransferase Required for Telomeric Silencing of Gene Expression. J Biol Chem 277:10753–10755. 10.1074/jbc.C200023200 [PubMed: 11805083]

Kundu S, Horn PJ, Peterson CL (2007) SWI/SNF is required for transcriptional memory at the yeast GAL gene cluster. Genes Dev 21:997–1004. 10.1101/gad.1506607 [PubMed: 17438002]

Kurdistani SK, Grunstein M (2003) Histone acetylation and deacetylation in yeast. Nat Rev Mol Cell Biol 4:276–284. 10.1038/nrml075 [PubMed: 12671650]

Landry J, Slama JT, Sternglanz R (2000) Role of NAD+ in the Deacetylase Activity of the SIR2-like Proteins. Biochem Biophys Res Commun 278:685–690. 10.1006/bbrc.2000.3854 [PubMed: 11095969]

Lemieux K, Gaudreau L (2004) Targeting of Swi/Snf to the yeast GAL1 UASG requires the Mediator, TAFIIs, and RNA polymerase II. EMBO J 23:4040–4050. 10.1038/sj.emboj.7600416 [PubMed: 15385957]

Lenstra TL, Benschop JJ, Kim T, et al. (2011) The Specificity and Topology of Chromatin Interaction Pathways in Yeast. Mol Cell 42:536–549. 10.1016/j.molcel.2011.03.026 [PubMed: 21596317]

Lenstra TL, Coulon A, Chow CC, Larson DR (2015) Single-Molecule Imaging Reveals a Switch between Spurious and Functional ncRNA Transcription. Mol Cell 60:597–610. 10.1016/j.molcel.2015.09.028 [PubMed: 26549684]

Li B, Carey M, Workman JL (2007) The Role of Chromatin during Transcription. Cell 128:707–719. 10.1016/j.cell.2007.01.015 [PubMed: 17320508]

Liang G, Klose RJ, Gardner KE, Zhang Y (2007) Yeast Jhd2p is a histone H3 Lys4 trimethyl demethylase. Nat Struct Mol Biol 14:243–245. 10.1038/nsmb1204 [PubMed: 17310254]

Liao Y, Wang J, Jaehnig EJ, et al. (2019) WebGestalt 2019: gene set analysis toolkit with revamped Uls and APIs. Nucleic Acids Res 47:W199–W205. 10.1093/nar/gkz401 [PubMed: 31114916]

Liu P, Song R, Elison GL, et al. (2017) Noise reduction as an emergent property of single-cell aging. Nat Commun 8:1–13. 10.1038/s41467-017-00752-9 [PubMed: 28232747]

Luo RX, Dean DC (1999) Chromatin Remodeling and Transcriptional Regulation. JNCI J Natl Cancer Inst 91:1288–1294. 10.1093/jnci/91.15.1288 [PubMed: 10433617]

Luo X, Song R, Acar M (2018) Multi-component gene network design as a survival strategy in diverse environments. BMC Syst Biol 12:85. 10.1186/s12918-018-0609-3 [PubMed: 30257679]

Martínez-Redondo P, Vaquero A (2013) The Diversity of Histone Versus Nonhistone Sirtuin Substrates. Genes and Cancer 4:148–163 [PubMed: 24020006]

Millar CB, Grunstein M (2006) Genome-wide patterns of histone modifications in yeast. Nat Rev Mol Cell Biol 7:657–666. 10.1038/nrm1986 [PubMed: 16912715]

Mumma JO, Chhay JS, Ross KL, et al. (2008) Distinct roles of galactose-1P in galactose-mediated growth arrest of yeast deficient in galactose-1P uridylyltransferase (GALT) and UDP-galactose 4′-epimerase (GALE). Mol Genet Metab 93:160–171. 10.1016/j.ymgme.2007.09.012 [PubMed: 17981065]

Murray SC, Haenni S, Howe FS, et al. (2015) Sense and antisense transcription are associated with distinct chromatin architectures across genes. Nucleic Acids Res 43:7823–7837. 10.1093/nar/gkv666 [PubMed: 26130720]

Nislow C, Ray E, Pillus L (1997) SET1, A Yeast Member of the Trithorax Family, Functions in Transcriptional Silencing and Diverse Cellular Processes. Mol Biol Cell 8:2421–2436. 10.1091/mbc.8.12.2421 [PubMed: 9398665]

Onge RPS, Mani R, Oh J, et al. (2007) Systematic pathway analysis using high-resolution fitness profiling of combinatorial gene deletions. Nat Genet 39:199–206. 10.1038/ngl948 [PubMed: 17206143]

Peng W, Liu P, Xue Y, Acar M (2015) Evolution of gene network activity by tuning the strength of negative-feedback regulation. Nat Commun 6:6226. 10.1038/ncomms7226 [PubMed: 25670371]

Peng W, Song R, Acar M (2016) Noise reduction facilitated by dosage compensation in gene networks. Nat Commun 7:1–8. 10.1038/ncommsl2959

Qian W, Ma D, Xiao C, et al. (2012) The Genomic Landscape and Evolutionary Resolution of Antagonistic Pleiotropy in Yeast. Cell Rep 2:1399–1410. 10.1016/j.celrep.2012.09.017 [PubMed: 23103169]

Rando OJ, Winston F (2012) Chromatin and Transcription in Yeast. Genetics 190:351–387. 10.1534/genetics.111.132266 [PubMed: 22345607]

Richmond TJ, Davey CA (2003) The structure of DNA in the nucleosome core. Nature 423:145–150. 10.1038/nature01595 [PubMed: 12736678]

Saldanha AJ (2004) Java Treeview--extensible visualization of microarray data. Bioinformatics 20:3246–3248. 10.1093/bioinformatics/bth349 [PubMed: 15180930]

Shanle EK, Andrews FH, Meriesh FI, et al. (2015) Association of Taf14 with acetylated histone H3 directs gene transcription and the DNA damage response. Genes Dev 29:1795–1800. 10.1101/gad.269977.115 [PubMed: 26341557]

Sharma VM, Tomar RS, Dempsey AE, Reese JC (2007) Histone Deacetylases RPD3 and HOS2 Regulate the Transcriptional Activation of DNA Damage-Inducible Genes. Mol Cell Biol 27:3199–3210. 10.1128/MCB.02311-06 [PubMed: 17296735]

Shivaswamy S, Iyer VR (2008) Stress-Dependent Dynamics of Global Chromatin Remodeling in Yeast: Dual Role for SWI/SNF in the Heat Shock Stress Response. Mol Cell Biol 28:2221–2234. 10.1128/MCB.01659-07 [PubMed: 18212068]

Soloveychik M, Xu M, Zaslaver O, et al. (2016) Mitochondrial control through nutritionally regulated global histone H3 lysine-4 demethylation. Sci Rep 6:37942. 10.1038/srep37942 [PubMed: 27897198]

Strahl BD, Grant PA, Briggs SD, et al. (2002) Set2 Is a Nucleosomal Histone H3-Selective Methyltransferase That Mediates Transcriptional Repression. Mol Cell Biol 22:1298–1306. 10.1128/MCB.22.5.1298-1306 [PubMed: 11839797]

Suka N, Suka Y, Carmen AA, et al. (2001) Highly Specific Antibodies Determine Histone Acetylation Site Usage in Yeast Heterochromatin and Euchromatin. Mol Cell 8:473–479. 10.1016/S1097-2765(01)00301-X [PubMed: 11545749]

Torchia TE, Hamilton RW, Cano CL, Hopper JE (1984) Disruption of regulatory gene GAL80 in Saccharomyces cerevisiae: effects on carbon-controlled regulation of the galactose/melibiose pathway genes. Mol Cell Biol 4:1521–1527. 10.1128/MCB.4.8.1521 [PubMed: 6092916]

van Leeuwen J, Boone C, Andrews BJ (2017) Mapping a diversity of genetic interactions in yeast. Curr Opin Syst Biol 6:14–21. 10.1016/j.coisb.2017.08.002 [PubMed: 30505984]

Vas AG, Andrews CA, Kirkland Matesky K, Clarke DJ (2007) In Vivo Analysis of Chromosome Condensation in Saccharomyces cerevisiae. Mol Biol Cell 18:557–568. 10.1091/mbc.e06-05-0454 [PubMed: 17151360]

Wan Y, Chen W, Xing J, et al. (2011) Transcriptome profiling reveals a novel role for trichostatin A in antagonizing histone chaperone Chzl mediated telomere anti-silencing. FEBS Lett 585:2519–2525. 10.1016/j.febslet.2011.06.036 [PubMed: 21763693]

Wang A, Kurdistani SK, Grunstein M (2002) Requirement of Hos2 histone deacetylase for gene activity in yeast. Science 298:1412–1414. 10.1126/science.1077790 [PubMed: 12434058]

Weinert BT, lesmantavicius V, Moustafa T, et al. (2014) Acetylation dynamics and stoichiometry in S accharomyces cerevisiae. Mol Syst Biol 10:716. 10.1002/msb.134766 [PubMed: 24489116]

Wu C (1997) Chromatin Remodeling and the Control of Gene Expression. J Biol Chem 272:28171–28174. 10.1074/jbc.272.45.28171 [PubMed: 9353261]

Yen K, Vinayachandran V, Pugh BF (2013) SWR-C and INO80 Chromatin Remodelers Recognize Nucleosome-free Regions Near+1 Nucleosomes. Cell 154:1246–1256. 10.1016/j.cell.2013.08.043 [PubMed: 24034248]

Yoon S, Qiu H, Swanson MJ, Hinnebusch AG (2003) Recruitment of SWI/SNF by Gcn4p Does Not Require Snf2p or Gcn5p but Depends Strongly on SWI/SNF Integrity, SRB Mediator, and SAGA. Mol Cell Biol 23:8829–8845. 10.1128/MCB.23.23.8829-9945 [PubMed: 14612422]

Yoshikawa K, Tanaka T, Ida Y, et al. (2011) Comprehensive phenotypic analysis of single-gene deletion and overexpression strains of Saccharomyces cerevisiae. Yeast 28:349–361. 10.1002/yea [PubMed: 21341307]

Zhang X, Wang X, Zhang Z, Cai G (2019) Structure and functional interactions of INO80 actin/Arp module. J Mol Cell Biol 11:345–355. 10.1093/jmcb/mjy062 [PubMed: 30388237]

Zhang Y (2001) Transcription regulation by histone methylation: interplay between different covalent modifications of the core histone tails. Genes Dev 15:2343–2360. 10.1101/gad.927301 [PubMed: 11562345]

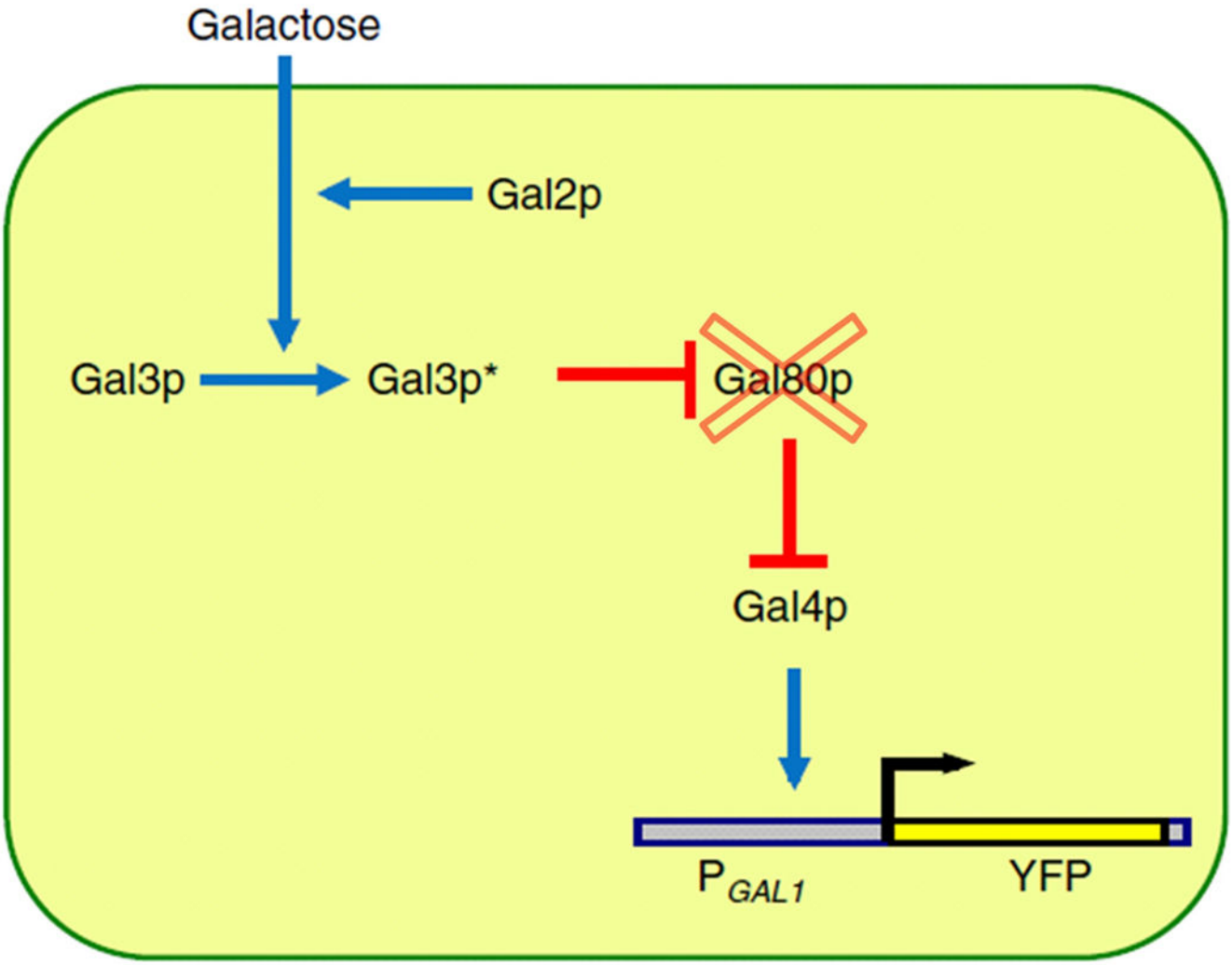

Fig 1. The galactose utilization network.

Network architecture built by the regulatory genes. The galactose-bound state of Gal3p is denoted by Gal3p*. Pointed blue arrows reflect activation and blunt red arrows reflect inhibition. Deletion of the *GAL80* gene leads to a constitutively active transcriptional network. YFP reports the activity of the network.

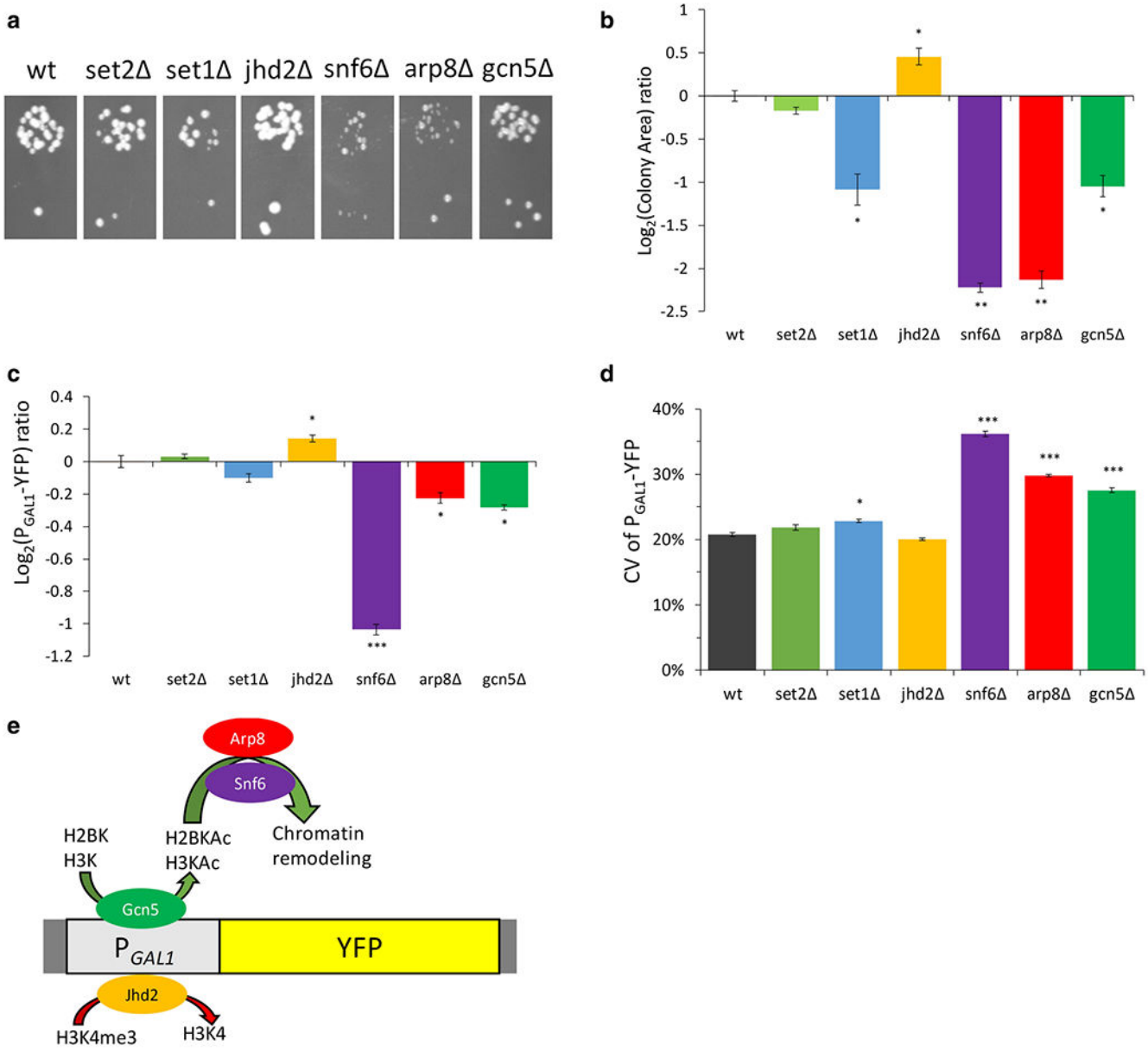

Fig 2. Variations in gene expression and vegetative growth in the chromatin regulator deleted strains.

a Representative image of the spotting growth assay of the indicated strains in SCD solid media after growth for 2 days at 30°C. **b** Quantification of the spotting-based growth assay based on measuring the area of single yeast colonies, **c** Relative YFP expression for each of the indicated strains over the wild type grown in SC media containing 0.1% mannose, **d** CV of p_{GAL1}-YFP expression of the indicated strains grown in SC media containing 0.1% mannose, **e** Model summarizing the roles of the chromatin regulators over the P_{GAL1}-YFP reporter system: green arrows represent processes favoring gene expression, red arrows represent processes inhibiting it. Error bars represent SEM (N=3-4). Statistical analysis was performed by a two-tailed t-test pairwise comparison between the wild type and each mutant's phenotype; *: $p<5{\cdot}10^{-2}$, **: $p<1{\cdot}10^{-3}$, ***: $p<1{\cdot}10^{-5}$.

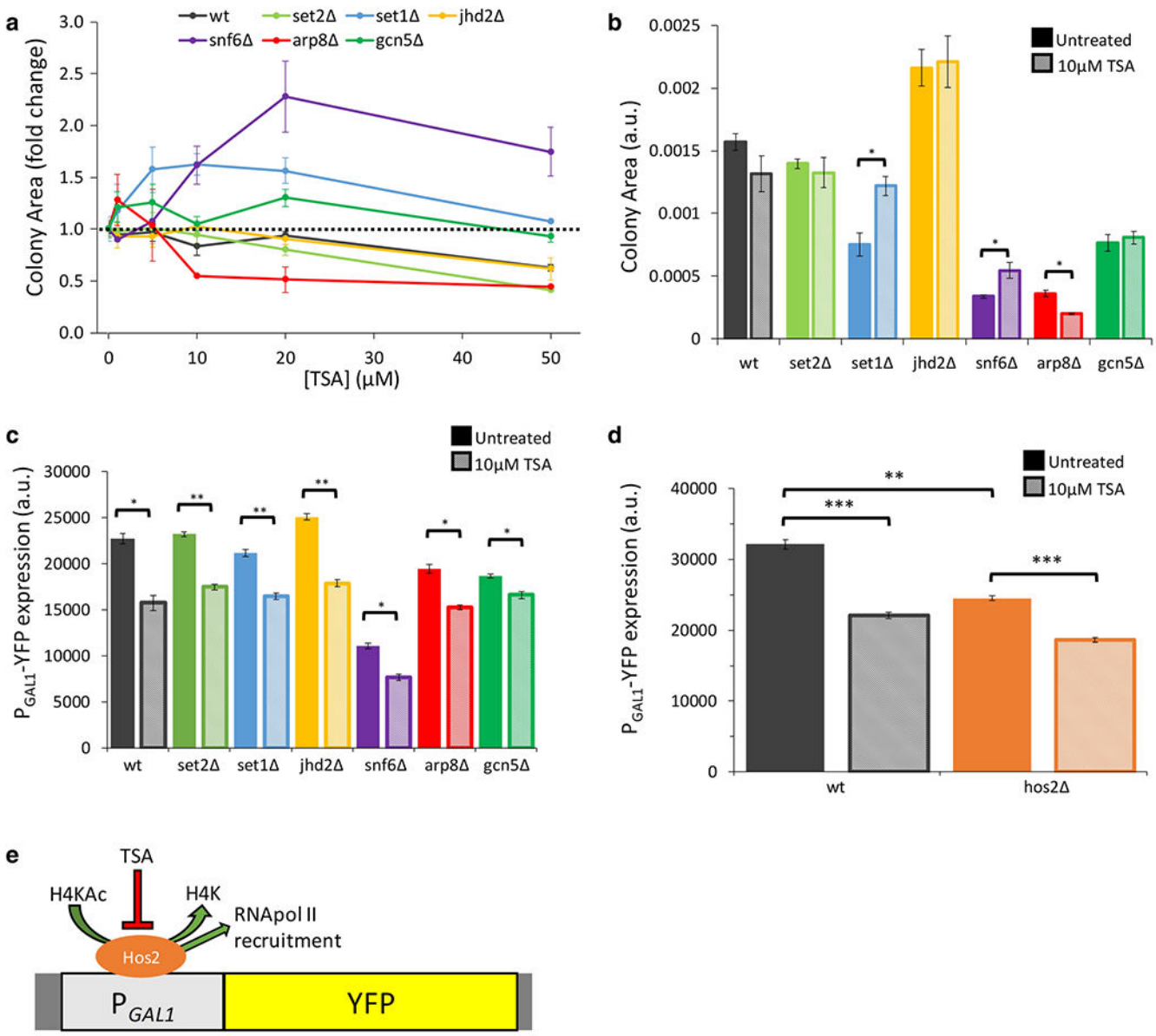

Fig 3. Effects of the chromatin regulator-deleted strains on gene expression and vegetative growth under Trichostatin A treatment.

a Drug effects on vegetative growth of constructed strains across a TSA concentration range (1, 5, 10, 20 and 50μM) in SCD solid media; all values were normalized to each strain's growth value measured in SCD solid media condition without drug, **b** Vegetative growth comparisons among the indicated strains with or without 10μM TSA treatment while grown on solid SCD media for 2 days at 30°C. **c-d** Mean YFP expression measured from each of the indicated strains treated with or without 10μM TSA. **e** Proposed mechanistic model to explain the gene expression reduction caused by the TSA treatment through Hos 2 inhibition: green arrows represent processes favoring gene expression, red arrows represent processes inhibiting it. Error bars represent SEM (N=3-4). Statistical analysis was performed

using a two-tailed t-test pairwise comparison of the phenotype measured with and without drug treatment for each strain, ns: not significant, *: $p<5\cdot10^{-2}$, **: $p<1\cdot10^{-3}$, ***: $p<1\cdot10^{-5}$.

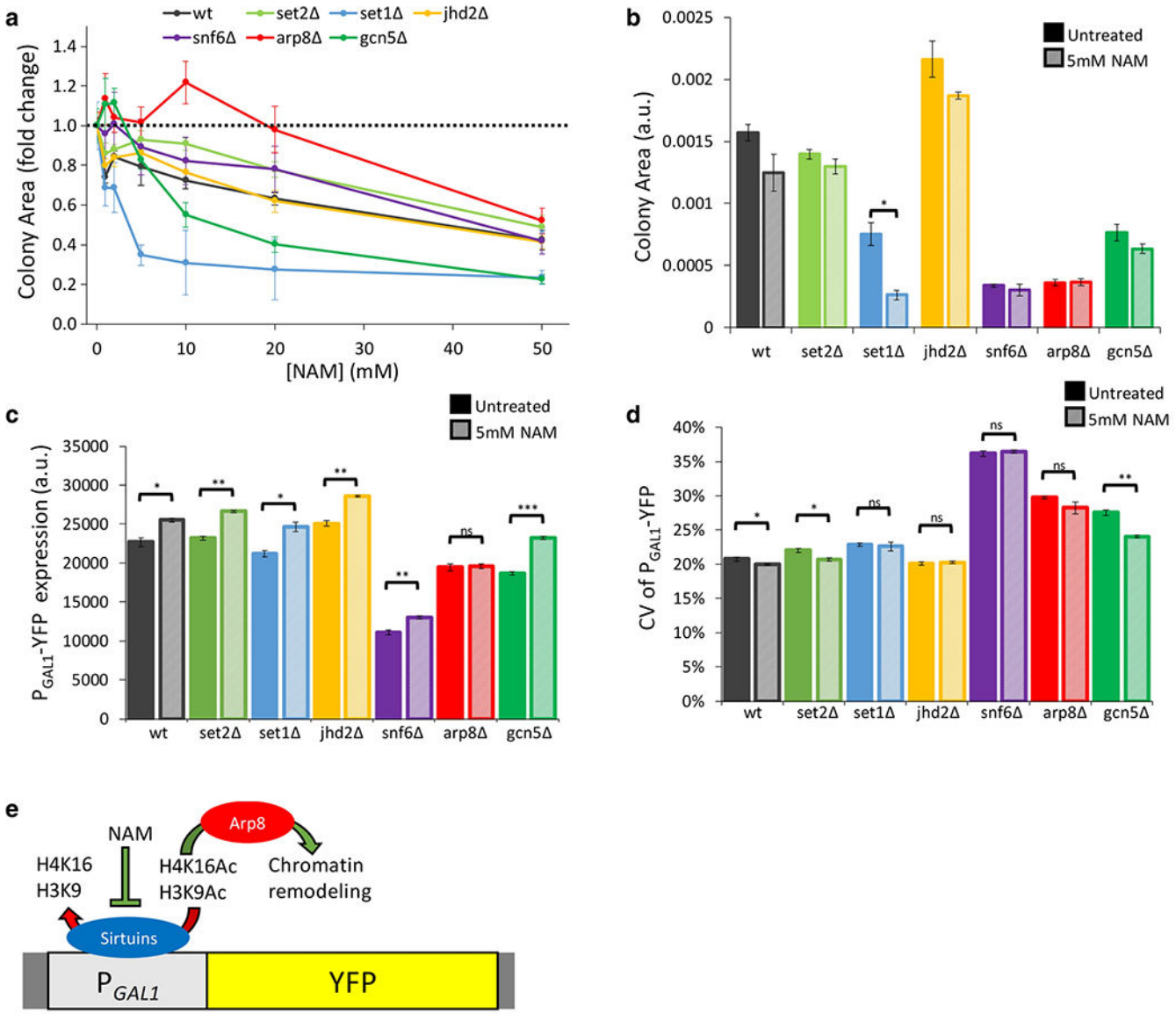

Fig 4. Effects of the chromatin regulator-deleted strains on gene expression and vegetative growth under Nicotinamide treatment.

a Drug effects on vegetative growth of constructed strains across a NAM concentration range (1, 2, 5, 10, 20 and 50mM) in SCD solid media; all values were normalized to each strain's growth value measured in SCD solid media condition without drug, **b** Vegetative growth comparisons among the indicated strains with or without 5mM NAM treatment while grown on solid SCD media for 2 days at 30°C. **c** Mean YFP expression measured from each of the indicated strains treated with or without 5mM NAM. **d** CV of YFP expression of each of the indicated strains with or without a 5mM NAM treatment, **e** Proposed mechanistic model to explain the gene expression increase caused by the NAM treatment through the inhibition of the silencing activity by sirtuins: green arrows represent processes favoring gene expression, red arrows represent processes inhibiting it. Error bars represent SEM (N=3-4). Statistical analysis was performed using a two-tailed t-test pairwise

comparison of the phenotype measured with and without drug treatment for each strain, ns: not significant, *: $p<5\cdot10^{-2}$, **: $p<1\cdot10^{-3}$, ***: $p<1\cdot10^{-5}$.

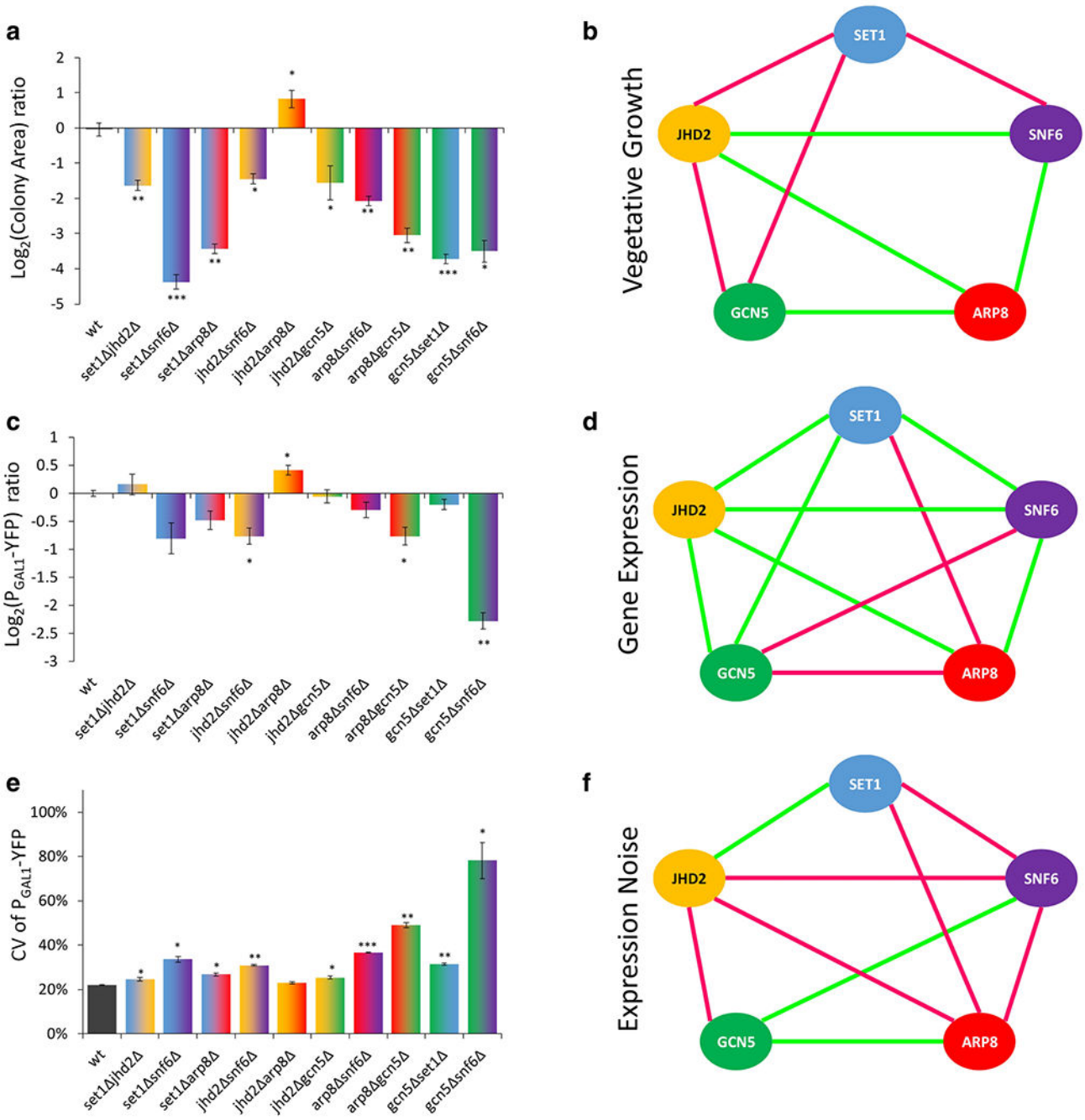

Fig 5. Genetic interactions between chromatin regulators in gene expression, noise and vegetative growth domains.

a Growth measurement by the spotting assay quantified by the mean colony area, **b** Computed as a function of vegetative growth, interaction network among the genes of interest, **c** Relative YFP expression for each of the indicated strains over the wild type grown in SC media containing 0.1% mannose, **d** Computed as a function of gene expression, interaction network among the genes of interest, **e** Mean CV of P_{GAL1}-driven YFP expression of the indicated strains growing in SC+0.1% mannose. **f** Computed as a function

of gene expression noise, interaction network among the genes of interest. In the interaction networks, the genes compose the network nodes and the detected interactions are represented by the lines; the color denotes the nature of the interaction (magenta: negative interaction, green: positive interaction). For differences from the multiplicative model and significance analysis with p-values, see Table S5. In the bar plots, error bars represent SEM (N=3-4). The statistical analysis was performed using a two-tailed t-test pairwise comparison between the wild type and each mutant's phenotype; *: $p<5\cdot10^{-2}$, **: $p<1\cdot10^{-3}$, ***: $p<1\cdot10^{-5}$.

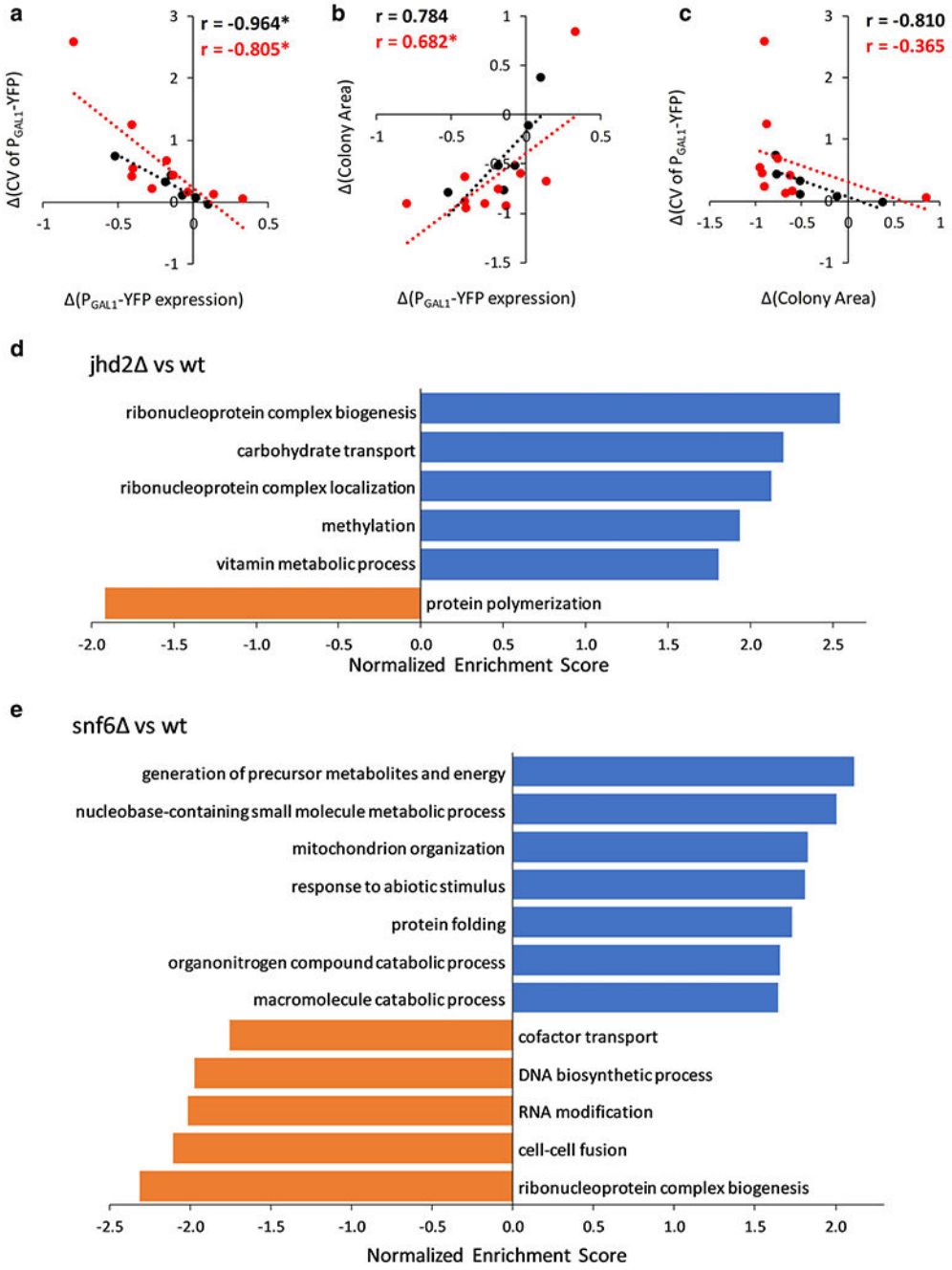

Fig 6. Correlations across phenotypes and enriched biological processes in mutant strains.

a-c Correlations of the deviations from the wild type strain for the indicated phenotypes measured from the single gene-deleted strains (black) and the double gene-deleted strains (red); Pearson's correlation coefficients (r) are shown in their corresponding color. * indicates significance of a correlation (α<0.05), based on the t-test. In **b**, the significance of the double-mutant strains' correlation is heavily influenced by an outlier data point, corresponding to the *jhd2Δarp8Δ* strain, **d-e** Normalized enrichment scores for gene sets from the Biological Process domain of the Gene Ontology after performing a GSEA on the

transcriptomic data of the indicated gene-deleted strains. Only gene sets with a False Discovery Rate (FDR)<0.05 are shown, after clustering gene sets by affinity propagation. Gene sets upregulated in gene-deleted strain are shown in blue, while downregulated gene sets are shown in orange.